FEBS Letters 527 (2002) 250–254 FEBS 26389

Identification of a basic surface area of the FADD death effector domain critical for apoptotic signaling

Markus Kaufmann[a,1], Damir Bozic[a,1], Christophe Briand[a], Jean-Luc Bodmer[b,2], Oliver Zerbe[c], Andreas Kohl[a], Jürg Tschopp[b], Markus G. Grütter[a,*]

[a] *Institute of Biochemistry, University of Zurich, Winterthurerstrasse 190, CH-8057 Zurich, Switzerland*
[b] *Institute of Biochemistry, University of Lausanne, BIL Biomedical Research Center, 155 chemin des Boveresse, CH-1066 Epalinges, Switzerland*
[c] *Institute of Pharmaceutical Sciences, Winterthurerstrasse 190, ETH Zurich, CH 8057 Zurich, Switzerland*

Received 18 June 2002; revised 22 July 2002; accepted 22 July 2002

First published online 19 August 2002

Edited by Gunnar von Heijne

Abstract Death effector domains (DEDs) are protein–protein interaction domains found in the death inducing signaling complex (DISC). Performing a structure-based alignment of all DED sequences we identified a region of high diversity in α-helix 3 and propose a classification of DEDs into class I DEDs typically containing a stretch of basic residues in the α-helix 3 region whereas DEDs of class II do not. Functional assays using mutants of Fas-associated death domain revealed that this basic region influences binding and recruitment of caspase-8 and cellular FLICE inhibitor protein to the DISC. **© 2002 Federation of European Biochemical Societies. Published by Elsevier Science B.V. All rights reserved.**

Key words: Death inducing signaling complex; Fas-associated death domain; Death effector domain; Homotypic interaction; Caspase-8; Cellular FLICE inhibitor protein

1. Introduction

Apoptosis is an important and tightly regulated process in the development and homeostasis of multi-cellular organisms [1]. Insufficient or excessive cell death has been shown to be associated with diseases [2,3]. In death receptor induced apoptosis, the activated receptors recruit the adapter protein FADD (Fas-associated death domain) through homotypic interactions between their death domain (DD) and the DD of FADD [4,5]. This assembly recruits procaspase-8, which binds through its tandem DEDs to the DED of FADD (FADD-DED) forming the death inducing signaling complex (DISC) [6]. In the DISC procaspase-8 is activated to process downstream executioner caspases. Antagonistic molecules like c-FLIP (cellular FLICE inhibitor protein)[7] regulate cell death at the level of the DISC. Two major splice variants, a short and a long form (c-FLIP$_S$ and c-FLIP$_L$) were described [8]. Both contain two DEDs that bind to FADD because of their similarity to the DEDs of procaspase-8/10. c-FLIP$_L$ in addition possesses an inactive caspase domain.

The formation of the DISC as well as of the apoptosome [9] is facilitated through homotypic domain interactions. These domains belong to the DD superfamily [10] comprising the DD, the DED, the caspase recruitment domain (CARD) and the pyrin domain [11] families. Although the sequence similarity of the DD superfamily is very low (5–25%), it shares an homotypic interaction mode and a common fold: an antiparallel six helical bundle with a Greek key topology [12]. Interactions between CARD–CARD [13] and DD–DD [14] have an electrostatic character, whereas DED–DED interactions so far were described to be of hydrophobic nature [15]. A large number of DEDs shares a conserved RXDL motif in the α-helix 6. In viral FLIP MC159, this motif is involved in apoptosis regulation [16].

Experiments described here reveal that in addition a basic surface area in DEDs is critical for apoptotic signalling.

2. Materials and methods

2.1. Sequence alignment and homology modeling

We performed a structure-based alignment using the coordinates of FADD-DED F25Y (PDB entry 1A1W [15]) as a template. A multiple sequence alignment of DEDs was performed using CLUSTAL X [17] which was manually corrected to primarily maintain the hydrophobic core. 1000 models were calculated for each aligned DED using MODELLER [18]. Models with the best stereochemistry, (PROCHECK [19]), were visualized using the program O [20]. When inappropriate interactions were observed further manual corrections of the alignment were made and a new set of models was calculated and checked. A final model for each DED was selected. The molecular surface was calculated and displayed using GRASP [21].

2.2. Mammalian and bacterial expression plasmids

Single site FADD mutants F25G, F25Y, double mutant K33,35Q and triple mutant K33,35N/R34S were produced by PCR using adequate PCR-primers. For mammalian expression, wild-type and mutant FADD were cloned into a pCR3 (Invitrogen) -derived vector using *Eco*RI and *Xho*I restriction sites. The resulting constructs encode human FADD (residues 2–208) with an N-terminal VSV-tag (MYTDIEMNRLGKEF) derived from the vesicular stomatitis virus glycoprotein. Constructs of human caspase-8-DED1+2 (residues 2–177), human c-FLIP-DED1+2 (residues 1–171) and human c-FLIP$_L$ [22] were cloned with an N-terminal Flag-tag (MDYKDDDDKEF). For *Escherichia coli* expression, the human FADD-DED (residues 1–83) K33,35Q mutant was subcloned into a pET21d(+) (Novagen) vector using *Nco*I an *Xho*I restriction sites. The resulting construct encodes the mutant protein with a C-terminal His-tag (LEHHHHHH).

2.3. Co-transfection

293T human embryonic epithelial kidney cells were co-transfected using the calcium phosphate method [23] with 7 μg of wild-type or

*Corresponding author. Fax: (41)-1-635 68 34.
E-mail address: gruetter@bioc.unizh.ch (M.G. Grütter).

[1] These authors contributed equally to the presented work.
[2] Present address: The Scripps Research Institute, Department of Molecular Biology - MB4, 10550 North Torrey Pines Road, La Jolla, CA 92037, USA.

0014-5793/02/$22.00 © 2002 Federation of European Biochemical Societies. Published by Elsevier Science B.V. All rights reserved.
PII: S0014-5793(02)03146-0

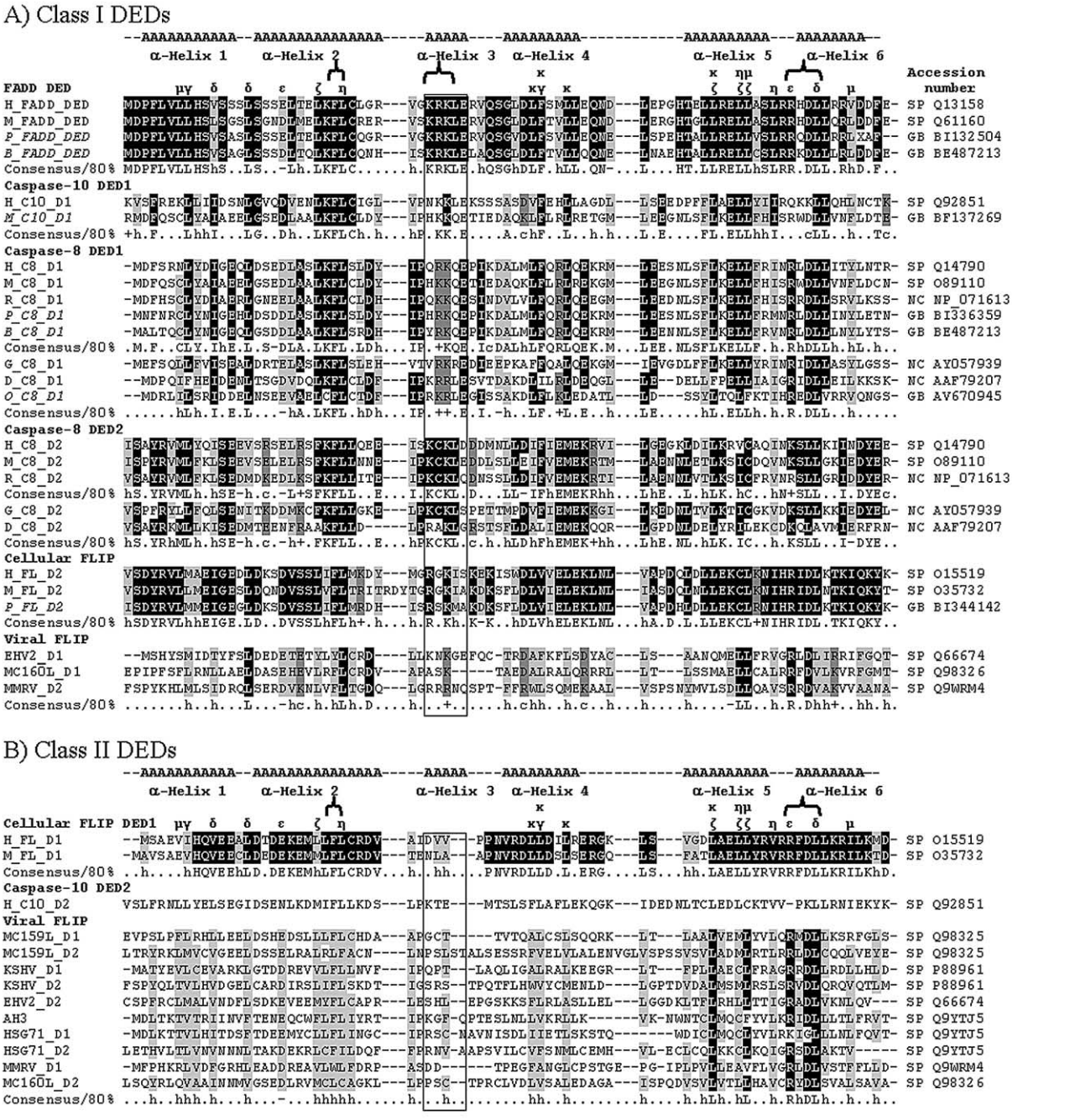

Fig. 1. Structure-based alignment of DEDs. A: Class I DEDs: presence of basic residues in α-helix 3 (boxed). B: Class II DEDs: absence of basic residues in α-helix 3 and α-helix 3 often shortened. Sequence names in italic were identified form the EST-database (http//www.ncbi.gov). Accession numbers and organisms are also listed in the figure. Consensus sequences are shown (h: hydrophobic, +: basic, −: acidic, c: charged). Positions of FADD-DED α-helices (A) are indicated. Greek letters correspond to intramolecular interactions of core residues of FADD-DED. Residue F25, the basic stretch and the RXDL motif are indicated by a brace.

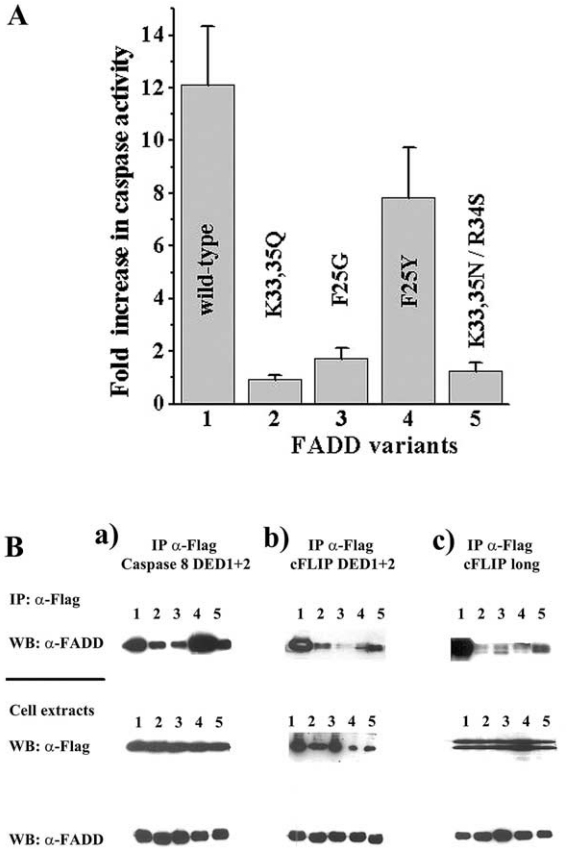

Fig. 2. A: Caspase-3 activity in presence of FADD variants. The caspase activity was given as fold increase in activity over that of cells transfected with an empty control vector and normalized to the total protein concentration. B: Binding of FADD variants to caspase-8-DED1+2, c-FLIP-DED1+2 and c-FLIP$_L$. 293T cells were co-transfected with FADD variants and (a) Flag-caspase-8-DED1+2, (b) Flag-c-FLIP-DED1+2 or (c) c-FLIP$_L$. After lysis, FADD was co-immunoprecipitated (IP α-Flag) with Flag-tagged binding partners (a–c) and immunoblotted using anti-FADD antibody (WB: α-FADD). The top panel demonstrates binding of FADD to caspase-8-DED1+2, c-FLIP-DED1+2, c-FLIP$_L$. The middle panel shows the level of caspase-8-DED1+2, c-FLIP-DED1+2 or c-FLIP$_L$ expression detected with an anti-Flag M2 antibody (WB: α-Flag). c-FLIP$_L$ appears as a double band due to partial processing. The bottom panel shows the level of FADD expression visualized with and anti-FADD antibody (WB: α-FADD). The FADD variants analyzed are 1: wild-type, 2: K 33,35Q, 3: F25G, 4: F25Y, 5: K33,35N/R34S.

mutant FADD plasmid, 7 μg of Flag-tagged caspase-8-DED1+2 or c-FLIP-DED1+2 or c-FLIP$_L$ [22] plasmid and 1 μg of enhanced green fluorescence protein expression plasmid to monitor transfection. 20 h after transfection cells were harvested and lysed in 170 μl of 0.2% Nonidet P40, 20 mM Tris/HCl, pH 7.4, 150 mM NaCl, 10% glycerol, protease inhibitor cocktail (Roche Biochemicals) by three freezing and thawing cycles.

2.4. Caspase activity assay

Caspase-3 activity was measured 18 h after incubation of the substrate as described by Bodmer et al. [24].

2.5. Co-immunoprecipitation

Wild-type and mutant FADD proteins were co-immunoprecipitated [25] with Flag-tagged partner DED molecules using anti-Flag M2 Agarose (Sigma) from 100 μl precleared post-nuclear cell lysate.

FADD expression was detected by Western blot with an anti-FADD antibody (BD Transduction Laboratories). Caspase-8-DED1+2, c-FLIP-DED1+2 and c-FLIP$_L$ expression were detected with an anti-Flag M2 antibody (Sigma). Antibodies were visualized using peroxidase conjugated goat anti-mouse IgG (Jackson) and Supersignal West Pico Chemoluminiescence Substrate (Pierce).

2.6. Expression of FADD-DED K33,35Q and NMR-spectroscopy

The ^{15}N labeled FADD-DED K33,35Q mutant was expressed in *E. coli* HMS174 strain (Novagen) as a soluble C-terminally His-tagged protein in M9-minimal medium [23] containing [^{15}N]NH_4Cl (Martek) as the nitrogen source and 100 μg/ml of ampicillin at 30°C. Induction was performed with 0.1 mM isopropyl-1-thio-β-D-galactopyranoside (MBI Fermentas) at an OD_{600nm} of 0.6 at 18°C. Bacteria were harvested 5 h after induction, centrifuged (4°C, 30 min, 4000×*g*), resuspended in 20 mM Tris–HCl, pH 8.0, 500 mM NH_4Cl, 5 mM β-mercaptoethanol and disrupted using a French press at 4°C. The lysate was cleared from debris by centrifugation (4°C, 30 min, 15 000×*g*) and loaded on Ni^{2+}-nitrilo-triacetate agarose (Qiagen) according to the suppliers instructions but exchanging NaCl with

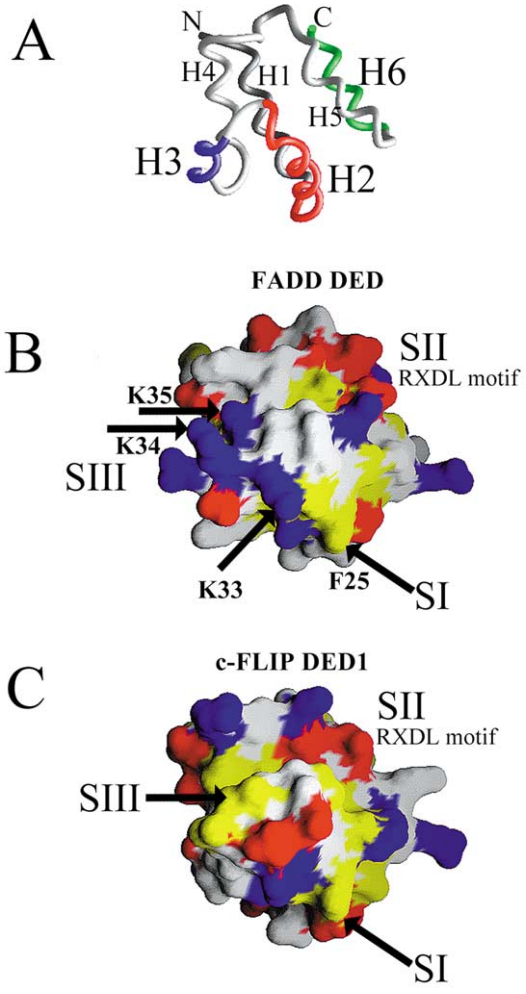

Fig. 3. A: Backbone representation of FADD-DED. The hydrophobic interaction surface (SI) in α-helix-2, the RXDL motif (SII) in α-helix 6 and the new interaction surface (SIII) in α-helix-3 are highlighted in red, green and blue respectively. B,C: Surface representation of DEDs. All molecules are in the same orientation as in (A). Basic side chains (R,K) are colored in blue, acidic side chains (D,E) are colored in red, hydrophobic side chains (A,V,L,I,M,F,P) are colored in yellow. B: Surface representation of a class I DED (wild-type FADD-DED). The basic surface SIII is typical for class I molecules. C: Surface representation of c-FLIP-DED1, a member of class II DEDs. The surface around residues corresponding to K33-K35 in FADD is hydrophobic (SIII). The hydrophobic surface SI and the RXDL motif (SII) are indicated. The figure was prepared with GRASP [21].

NH_4Cl and including 5 mM β-mercaptoethanol. The protein was eluted with 40 mM NH_4OAc, pH 4.0, 50 mM NH_4Cl, 5 mM β-mercaptoethanol and concentrated to 0.5 mM using a Centricon YM-3 (Amicon). 10% D_2O was added to the protein solution. A $^1H^{15}N$ heteronuclear single quantum coherence (HSQC) spectrum [26] was recorded at 280 K on a DRX-500 Bruker Avance instrument using a standard sensitivity-enhanced pulse sequence [27] with pulsed-field gradients [28]. Thirty-two free-induction decays were averaged for each increment. Proton chemical shifts were referenced with respect to the water frequency [29] and the ^{15}N chemical shift scale was referenced indirectly to liquid ammonia [30].

3. Results and discussion

Our structure-based alignment analysis using the available DED sequences provided homology model structures for all known DED containing components of the DISC. The main differences between the various model structures were located in α-helix 3, which resulted from the criterion to maintain the hydrophobic core of the domain. The analysis revealed two distinct classes of DED structures. Members of class I share high sequence similarity with FADD-DED and possess basic residues in α-helix 3 (residues 33–35 in FADD). The DED of FADD, both DEDs of caspase-8, the N-terminal DED of caspase-10 and the C-terminal DED of c-FLIP (Fig. 1) belong to this class. Members of the class II do not contain basic residues at positions 33–35, and in addition α-helix 3 is shorter or missing in most of them. The class II includes the C-terminal DED of caspase-10 and the N-terminal DED of c-FLIP as well as most of the viral DEDs (Fig. 1).

The role of the basic stretch in class I DEDs was assessed with variants of FADD-DED. The functionality of wild-type and mutant FADD molecules were assayed. Expression of functional FADD leads to the activation of caspase-8, which subsequently activates caspase-3. Functionality was measured using a caspase-3 activity assay (Fig. 2A). Binding of FADD variants to procaspase-8 and c-FLIP was analyzed by co-immunoprecipitation (Fig. 2B). The experiments show that K33,35Q and K33,35N/R34S FADD mutants exhibit low background level caspase-3 activity and reduced binding to c-FLIP and caspase-8 like FADD F25G mutant. These results imply that not only the hydrophobic surface region around F25 (SI; Fig. 3) but also the basic region K33R34K35 of FADD-DED (SIII, Fig. 3) is important for the apoptosis signaling and suggests that electrostatic forces are also involved in DED interactions.

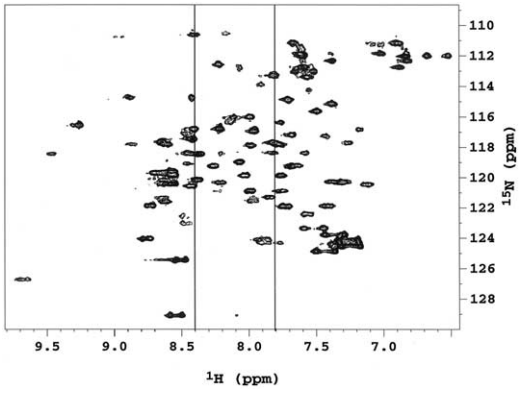

Fig. 4. [^{15}N,^1H]HSQC spectrum of FADD-DED K33,35Q. The proton chemical shift range between 7.8 and 8.4 ppm, typically encountered for amide protons in unstructured proteins, is indicated by vertical lines [34]. Peaks doubling indicate the existence of an asymmetric dimer of FADD-DED in solution.

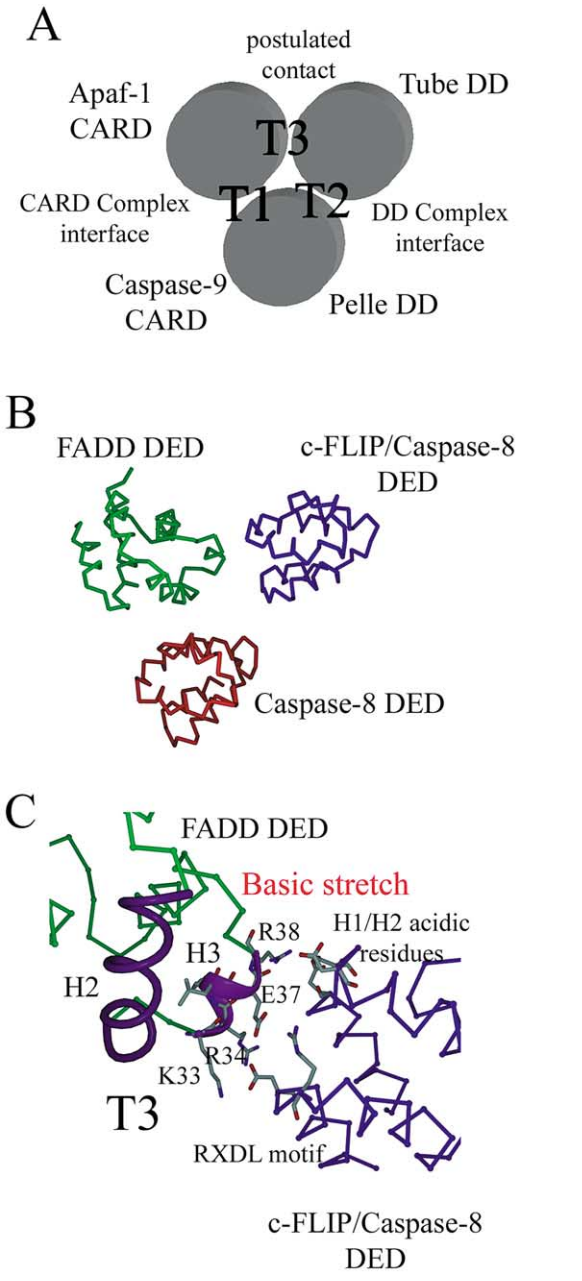

Fig. 5. Schematic representation of the proposed trimer model [10]. A: The caspase-9 CARD of the Apaf-1/caspase-9 CARD complex and the Pelle DD from the Pelle/Tube DD complex were superimposed. T1 and T2 interfaces are experimentally observed in the crystal structures of the complexes and a new intermolecular contact T3 is predicted. B: CARDs and DDs are replaced in this model by DEDs, with FADD-DED (green), caspase-8-DED (red) and c-FLIP or caspase-8-DED (blue). C: The resulting T3 contact is presented. α-Helix 3 (H3) (residues K33 to R38) interact with the RXDL motif and the acidic region from α-helices 1 and 2 of another domain. Figures were prepared with DINO (http://www.dino3d.org).

Comparative levels of caspase-3 activation are observed for wild-type and the F25Y FADD mutant. Surprisingly F25Y FADD binds full-length procaspase-8 equally strong as wild-type FADD [15] while the interaction with c-FLIP is reduced. This indicates, that c-FLIP binds in a different man-

ner or with different affinities to FADD than procaspase-8 (Fig. 2B).

In order to show that mutant FADD molecules (mutations in the region 33–35) are folded proteins, the DED of the FADD K33,35Q mutant was expressed in *E. coli* and analyzed by 2D-NMR $^{1}H^{15}N$ spectroscopy. In the HSQC spectrum (Fig. 4) signals are spread over a broad range of chemical shifts, typical for a globular and folded protein [31].

All DED homology models possess a characteristic hydrophobic surface (SI, Fig. 3B) formed by conserved residues around a phenylalanine in α-helix 2 (F25 in FADD) [15]. In most DEDs, an electrostatic surface around the RXDL motif in α-helix 6 (SII, Fig. 3B) is also present [16]. In contrast, the positively charged surface area around α-helix 3 (SIII, Fig. 3B) is only shared by DEDs of class I. This surface area is uncharged in class II DEDs (Fig. 3C).

Weber et al. [10,32] proposed a structural model for DD interaction in apoptotic signaling (Fig. 5A). Because DED and DD might have evolved from the CARD family [10], we superimposed DEDs onto their postulated DD trimer model [10] and we obtained an arrangement as shown in Fig. 5B. In this model the above-mentioned DED surfaces are forming the DED–DED contacts. Our mutagenesis studies presented here and recent mutagenesis results in the literature [16] are strong experimental support for the interaction surface T3 in the model (Fig. 5A). The T3 contact is made by the α-helix 3 region of FADD-DED with K33-R38 contacting another partner DED in the RXDL region (Fig. 5C). Recently Garvey et al. [16] analyzed mutants of v-FLIP MC159 for their binding to FADD and for their capability to inhibit apoptosis. They show that mutations in the RXDL motif of either domain result in the loss of inhibition of apoptosis.

Our findings contribute to the understanding of intermolecular interactions between DEDs. They support the view that more than a single surface area is required for binding of partner molecules and emphasizes the role of α-helix 3. Recently a procaspase-10 molecule mutated in α-helix 3 of the C-terminal DED (M147T) was discovered in patients with gastric cancer [33]. This tumor-derived procaspase-10 mutant is believed to be responsible for a lower apoptotic activity function disrupting apoptosis. The analysis of the recently postulated trimer model [10] in view of pure DED interactions does not only explain recent mutagenesis data but also correlates the RXDL motif of DED partners to the basic stretch of α-helix 3 in FADD.

Acknowledgements: Financial support by the Swiss National Science Foundation to M.G.G. and to J.T. and financial support to M.G.G. from the Baugartenstiftung (CH-8022 Zürich) is gratefully acknowledged.

References

[1] Heemels, M.T. (2000) Nature 407, 769–816.
[2] Zornig, M., Hueber, A., Baum, W. and Evan, G. (2001) Biochim. Biophys. Acta. 1551, F1–F37.
[3] Roshal, M., Zhu, Y. and Planelles, V. (2001) Apoptosis 6, 103–116.
[4] Chinnaiyan, A.M., Tepper, C.G., Seldin, M.F., O'Rourke, K., Kischkel, F.C., Hellbardt, S., Krammer, P.H., Peter, M.E. and Dixit, V.M. (1996) J. Biol. Chem. 271, 4961–4965.
[5] Bodmer, J.L., Schneider, P. and Tschopp, J. (2002) Trends Biochem. Sci. 27, 19–26.
[6] Walczak, H. and Sprick, M.R. (2001) Trends Biochem. Sci. 26, 452–453.
[7] Rasper, D.M., Vaillancourt, J.P., Hadano, S., Houtzager, V.M., Seiden, I., Keen, S.L., Tawa, P., Xanthoudakis, S., Nasir, J., Martindale, D., Koop, B.F., Peterson, E.P., Thornberry, N.A., Huang, J., MacPherson, D.P., Black, S.C., Hornung, F., Lenardo, M.J., Hayden, M.R., Roy, S. and Nicholson, D.W. (1998) Cell Death Differ. 5, 271–288.
[8] Tschopp, J., Irmler, M. and Thome, M. (1998) Curr. Opin. Immunol. 10, 552–558.
[9] Acehan, D., Jiang, X., Morgan, D.G., Heuser, J.E., Wang, X. and Akey, C.W. (2002) Mol. Cell 9, 423–432.
[10] Weber, C.H. and Vincenz, C. (2001) Trends Biochem. Sci. 26, 475–481.
[11] Fairbrother, W.J., Gordon, N.C., Humke, E.W., O'Rourke, K.M., Starovasnik, M.A., Yin, J.P. and Dixit, V.M. (2001) Protein Sci. 10, 1911–1918.
[12] Sukits, S.F., Lin, L.L., Hsu, S., Malakian, K., Powers, R. and Xu, G.Y. (2001) J. Mol. Biol. 310, 895–906.
[13] Qin, H., Srinivasula, S.M., Wu, G., Fernandes-Alnemri, T., Alnemri, E.S. and Shi, Y. (1999) Nature 399, 549–557.
[14] Xiao, T., Towb, P., Wasserman, S.A. and Sprang, S.R. (1999) Cell 99, 545–555.
[15] Eberstadt, M., Huang, B., Chen, Z., Meadows, R.P., Ng, S.C., Zheng, L., Lenardo, M.J. and Fesik, S.W. (1998) Nature 392, 941–945.
[16] Garvey, T.L., Bertin, J., Siegel, R.M., Wang, G.H., Lenardo, M.J. and Cohen, J.I. (2002) J. Virol. 76, 697–706.
[17] Thompson, J.D., Higgins, D.G. and Gibson, T.J. (1994) Nucleic Acids Res. 22, 4673–4680.
[18] Sali, A. and Blundell, T.L. (1993) J. Mol. Biol. 234, 779–815.
[19] Laskowski, R.A., MacArthur, M.W., Moss, D.S. and Thornton, J.M. (1993) J. Appl. Crystallogr. 26, 283–291.
[20] Jones, T.A., Zou, J.Y., Cowan, S.W. and Kjeldgaard, M. (1991) Acta Crystallogr. A47, 110–119.
[21] Nicholls, A., Sharp, K.A. and Honig, B. (1991) Proteins 11, 281–296.
[22] Irmler, M., Thome, M., Hahne, M., Schneider, P., Hofmann, K., Steiner, V., Bodmer, J.L., Schroter, M., Burns, K., Mattmann, C., Rimoldi, D., French, L.E. and Tschopp, J. (1997) Nature 388, 190–195.
[23] Sambrook, J., Fritsch, E.F. and Maniatis, T. (1989), Molecular Cloning, Cold Spring Harbor Laboratory Press, Cold Spring Harbor, NY.
[24] Bodmer, J.L., Holler, N., Reynard, S., Vinciguerra, P., Schneider, P., Juo, P., Blenis, J. and Tschopp, J. (2000) Nat. Cell Biol. 2, 241–243.
[25] Bodmer, J.L., Burns, K., Schneider, P., Hofmann, K., Steiner, V., Thome, M., Bornand, T., Hahne, M., Schroter, M., Becker, K., Wilson, A., French, L.E., Browning, J.L., MacDonald, H.R. and Tschopp, J. (1997) Immunity 6, 79–88.
[26] Bodenhausen, G. and Ruben, D.J. (1980) Chem. Phys. Lett. 69, 185–189.
[27] Palmer, A.G., Cavanagh, J., Wright, P.E. and Rance, M. (1991) J. Magn. Reson. 93, 151–170.
[28] Kay, L.E., Keifer, P. and Saarien, T. (1992) J. Am. Chem. Soc. 114, 10663–10665.
[29] Cavanagh, J., Fairbrother, W.J., Palmer, A.G. and Skelton, N.J. (1996), Protein NMR Spectroscopy: Principles and Practice, Academic Press, London.
[30] Live, D.H., Davis, D.G., Agosta, W.C. and Cowburn, D. (1984) J. Am. Chem. Soc. 106, 6104.
[31] Wishart, D.S., Sykes, B.D. and Richards, F.M. (1991) J. Mol. Biol. 222, 311–333.
[32] Weber, C.H. and Vincenz, C. (2001) FEBS Lett. 492, 171–176.
[33] Park, W.S., Lee, J.H., Shin, M.S., Park, J.Y., Kim, H.S., Kim, Y.S., Lee, S.N., Xiao, W., Park, C.H., Lee, S.H., Yoo, N.J. and Lee, J.Y. (2002) Oncogene 21, 2919–2925.
[34] Bundi, A. and Wüthrich, K. (1979) Biopolymers 18, 285–297.